

Schwinger dark matter production

Mar Bastero-Gil,^{1,*} Paulo B. Ferraz,^{1,2,†} Lorenzo Ubaldi,^{3,4,‡} and Roberto Vega-Morales^{1,§}

¹*Departamento de Física Teórica y del Cosmos and CAFPE,*

Universidad de Granada, Campus de Fuentenueva, E-18071 Granada, Spain

²*Universidade de Coimbra, Faculdade de Ciências e Tecnologia da Universidade de Coimbra and CFisUC, Rua Larga, 3004-516 Coimbra, Portugal*

³*Jožef Stefan Institute, Jamova 39, 1000 Ljubljana, Slovenia*

⁴*Institute for Fundamental Physics of the Universe (IFPU), Via Beirut 2, 34014 Trieste, Italy*

Building on recently constructed inflationary vector dark matter production mechanisms as well as studies of magnetogenesis, we show that a *dark* Schwinger mechanism can generate the observed dark matter relic abundance. This mechanism can take place during inflation and/or after reheating and leads to a feebly interacting dark sector which is comprised of dark fermions and/or scalars which can be as light as $\sim 10\text{ MeV}$ and as heavy as $\sim 10^{10}\text{ GeV}$ depending on how the (unknown) Schwinger current redshifts after inflation. The background dark electric field is generated during inflation and can continue sourcing Schwinger pair production after reheating until the dark charged particles become non-relativistic. The dark matter can interact very weakly via the exchange of ultralight dark photons and has a power spectrum which is peaked at very small scales, thus evading potential isocurvature constraints. We emphasize that this mechanism is viable even near the conformal limit where (purely) gravitational particle production is negligible. Thus dark matter can be produced solely via the Schwinger effect even with a very weak electric force.

INTRODUCTION

The nature and production mechanism of dark matter is still unknown. Significant research effort has been put into candidates like weakly interacting massive particles, axions, sterile neutrinos, but we have seen no experimental evidence for them yet [1]. This motivates studying alternative candidates as well. One class which has received considerable attention in the recent past is that of dark photon dark matter, produced via non-thermal mechanisms [2–17] where the dark photon is associated with a dark $U(1)_D$ abelian gauge theory. At some point before matter radiation equality the dark photon must become massive, even if very light, in order to provide a cold (non-relativistic) dark matter candidate. However, it has been argued [18] that the formation of vortices in these scenarios spoils the possibility of the dark photon being dark matter¹. One can consider adding scalar and/or fermion fields charged under the $U(1)_D$ to the dark sector, of which the dark photon is the gauge boson. Utilizing one of the dark photon production mechanisms above, all that is needed is a way to transfer the energy density from the dark photon to the dark ‘dark electrons’² which can then constitute the dark matter.

Such a ‘dark QED’ setup was studied in [20] which utilized the mechanism of [2] to generate a dark electric field composed of the longitudinal mode of the (massive)

dark photon which is produced via inflationary fluctuations. While the modes are produced during inflation, the cold vector condensate, which can be treated as a classical dark electric field, only forms in the radiation dominated epoch when the vector momentum modes re-enter the horizon [2]. Furthermore, since the dark electric field which is produced is not very large compared to Hubble, this mechanism requires efficient transfer of the dark sector energy density from the dark photon to the dark electrons which requires the dark sector to thermalize in order to produce enough dark matter. It was shown [20] how via various QED processes such as electromagnetic cascades, and plasma dynamics, as well as a subdominant contribution from Schwinger pair production, the dark sector can thermalize with itself while remaining decoupled from the visible thermal bath. In this case the amount of dark electrons today is determined by the interplay between the various thermalization processes in the dark sector and one obtains a relic abundance which matches the one observed for dark matter in the mass range from 50 MeV to 30 TeV . In order to achieve thermalization the dark $U(1)_D$ gauge coupling cannot be too small, roughly $\gtrsim 10^{-3}$. Furthermore, as in [2], the dark photon must be massive for the whole of its cosmological evolution including during inflation.

We consider a similar dark QED scenario with the same field content as in [20], but instead where the dark electric field is generated by the mechanism proposed in [6, 13] which is based on an axion like coupling between the gauge field and the inflaton. Compared to the longitudinal mode production mechanism [2] discussed above, the mechanism utilized here produces much larger coherent dark electric fields already during inflation via one

¹ However, these constraints can be softened in some dark photon dark matter scenarios [19]

² We will generically refer to both scalars and fermions charged under the dark $U(1)_D$ as dark electrons.

of the *transverse* vector modes. Since it is the transverse mode which is produced, this mechanism also works in the massless dark photon case. Once formed these background fields can then source Schwinger pair production during and, in principle, after inflation.

After reheating, the large electric fields continue to accelerate the dark electrons which have been pair produced. This imposes a stringent upper bound on the dark gauge coupling coming from the condition that the dark electrons become non-relativistic by the time of matter radiation equality. As we'll see, this guarantees that we are always in the regime where the dark sector does *not* thermalize with itself. However, in this case the dark sector does not need to thermalize since, with the much larger electric fields, enough dark electrons can be produced solely via Schwinger pair production to reproduce the dark matter relic abundance. In the thermalization case discussed above, there is also Schwinger pair production taking place, but any initial seed of dark electrons coming from Schwinger production is washed out by the more dominant thermalization effects [20].

In the vector production mechanism considered in [2, 20] one can have large enough gauge couplings to thermalize, but yet not violate the non-relativistic condition. This is because in this case the dark electric field is much smaller so the electric force which accelerates the dark electrons is much weaker than in the mechanism considered here [6, 13]. This leads us to conclude that mechanisms which give weak dark electric fields can thermalize and in fact they must thermalize in order to produce enough dark electrons to constitute the dark matter. Mechanisms with stronger dark electric fields require much smaller gauge couplings to not violate the non-relativistic condition leading to no thermalization in the dark sector. In this case however the much larger dark electric field can generate the necessary amount of dark matter solely via the Schwinger effect.

At the end of inflation and the onset of reheating, which we assume instantaneous, we have an energy density in the dark sector which is dominated by the dark electric field along with a tiny seed of Schwinger produced dark electrons. Schwinger production continues after reheating, but becomes inefficient once the dark electrons become non-relativistic. At that point the energy density in the Schwinger produced dark electrons is still smaller than that of the dark electric field. However, from then on the dark electrons begin redshifting like non-relativistic matter and come to dominate the dark sector energy density by the time of matter-radiation equality. Thus, the final relic abundance is set by the balance between Schwinger pair production and redshifting effects. Following this evolution we show that Schwinger produced dark electrons can reproduce the observed dark matter relic abundance for masses potentially as light as $\sim 10 \text{ MeV}$ and as heavy as $\sim 10^{10} \text{ GeV}$ for Hubble scales at the end of inflation in the range $10^8 - 10^{14} \text{ GeV}$. We expect the

dark electrons to have a power spectrum peaked around the same scales as the dark photon. This was shown to be at very small scales [13], thus evading constraints on isocurvature coming from measurements of the CMB.

Interestingly, and perhaps surprisingly, the dark Schwinger production mechanism is viable even in the weak dark electric field regime where backreaction effects can be neglected. This depends crucially on the fact that it occurs in an expanding background and is not possible in flat space where strong fields are required for efficient Schwinger production. This feature of the weak field regime in de-Sitter space was explored in various studies [21–29] examining magnetogenesis. In these studies the conserved Schwinger current during inflation was computed for both scalars [24] and fermions [23]. We adapt these results to study the evolution of the energy density of the produced dark sector particles averaged over space in order to estimate the parameter space where we can obtain the correct dark matter abundance.

We also emphasize that conformal invariance must be broken during inflation to generate particles. In inflationary Schwinger production the conformal symmetry breaking comes from the background electric field (which can be generated in various ways). This breaking of conformal invariance ‘leaks’ into the matter sector via the Schwinger mechanism allowing for production of charged particles even in the absence of conformal breaking in the fermion and scalar sectors. In this way even massless fermions or conformally coupled massless scalars, which would not be produced by gravitational particle production due to a changing metric [30, 31], can still be produced during inflation via the Schwinger effect.

Finally, we comment that part of our analysis relies on the Schwinger current after reheating, but to our knowledge there are no studies of Schwinger production in a Friedmann-Robertson-Walker (FRW) background which can be applied to epochs of radiation and matter domination. Thus, with the aim of simply gaining intuition and an estimate of the amount of dark particles which can be produced, in this study we assume that the electrical conductivity in the dark sector at the end of inflation either remains constant or redshifts at some rate after reheating. We leave a detailed study of the Schwinger mechanism in a generic FRW background and more precise estimate of the dark matter parameter space as well as power spectrum to ongoing work.

DARK SCHWINGER PRODUCTION

In this section we first review the relevant aspects of the Schwinger mechanism needed for production of dark charged particles in the expanding universe. Details of the results summarized and applied to dark QED here can be found in [22–24], which studied the Schwinger effect in deSitter space, relevant for the period of inflation.

We consider a dark $U(1)_D$ gauge field during inflation with gauge coupling g_D which couples to dark charged fermions and/or scalars which we label χ . We assume χ to have dark charge $Q_\chi = 1$ and to be a singlet under the Standard Model. In analogy with standard QED,

$$S = \int d^4x \sqrt{-g} \left(-\frac{1}{4} F^{\mu\nu} F_{\mu\nu} + \mathcal{L}_{\text{charged}}(A_\mu, \chi) \right), \quad (1)$$

where for charged scalars we have,

$$\mathcal{L}_{\text{charged}}^{\text{scalar}} = -|D_\mu \chi|^2 - (m_\chi^2 + \xi_R R) |\chi|^2, \quad (2)$$

and for charged fermions,

$$\mathcal{L}_{\text{charged}}^{\text{fermion}} = \bar{\chi} (i\gamma^\mu D_\mu - m_\chi) \chi. \quad (3)$$

Here $F_{\mu\nu} = \partial_\mu A_\nu - \partial_\nu A_\mu$, while $D_\mu = \partial_\mu + ig_D A_\mu + \Gamma_\mu$, where Γ_μ is the spinor connection (which is zero in the scalar case) and R is the Ricci scalar. We parametrize the background de-Sitter spacetime by the Friedmann-Robertson-Walker metric with $ds^2 = -dt^2 + a^2(t) d\vec{x}^2$ and the convention $\epsilon^{0123} = 1/\sqrt{-g}$.

In order to isolate the Schwinger production from the possible gravitational production [30, 31], we consider the conformal limit where $m_\chi/H \ll 1$ with H the Hubble parameter during inflation and $\xi_R = 1/6$ for the scalar case in Eq. (2). While we can neglect m_χ during inflation in this limit, at some point in its cosmic evolution χ must obtain a mass to eventually become non-relativistic, as required for cold dark matter. We also assume for now a constant classical dark electric field during inflation and discuss in the next section how it can be generated.

The electric field has a direction, which we take to be along the z axis, and will generate a current of charged particles via the Schwinger effect. Calculation of the current is challenging and requires renormalization, but has been performed both for scalars [22] and fermions [23] in $3+1$ de-Sitter space. Following the notation of [22], we can write the electric field in the z direction as $E_i = aE\delta_{iz}$ with E constant and the current as $\langle J_i \rangle = aJ\delta_{iz}$. In both cases a is the comoving scale factor which appears in the metric, and we refer to the quantities E and J as the physical electric field and physical current respectively. We can then define the electrical conductivity, and its dimensionless counterpart, as

$$\sigma = \frac{J}{E}, \quad \bar{\sigma} \equiv \frac{\sigma}{H}. \quad (4)$$

As we'll see below, with the conductivity as input we can compute the energy density of the Schwinger produced charged particles during inflation in terms of the energy density of the dark E -field.

To estimate the energy density ρ_χ of dark charged particles we assume they form a perfect fluid whose evolution during inflation we can describe as [27],

$$\dot{\rho}_\chi + nH\rho_\chi = \langle E \cdot J \rangle = \sigma \langle E^2 \rangle. \quad (5)$$

Here $\langle E^2 \rangle$ represents the spacial average of the magnitude squared of the dark electric field, We also have $n = 3$ for the non-relativistic case and $n = 4$ for the relativistic case while the overdot denotes a derivative with respect to cosmic time t . This evolution equation can be derived from the energy momentum tensor and expresses energy conservation where $\langle E \cdot J \rangle$ acts as a source term for the χ energy density. A corresponding term, with the opposite sign, appears in the evolution equation for the energy density of the dark electric field. This must be sourced during inflation, as we discuss in the next section, but is depleted by the $-\sigma \langle E^2 \rangle$ term, which is due to the Schwinger production³. We work in the small conductivity regime where,

$$0 < \bar{\sigma} \ll 1, \quad (6)$$

so we can neglect the depleting term in the evolution equation for the energy density of the dark electric field and treat Eq. (5) for ρ_χ as decoupled. If m_χ/H is not small during inflation or the dark scalar has a non-conformal coupling to gravity there should be an additional term present in Eq. (5) due to gravitational particle production [30, 31]. As mentioned above, we assume we are near the conformal limit where this production is negligible and leave a study of the conformal breaking case where $m_\chi/H > 1$ to a companion paper [32].

During inflation it is convenient to rewrite Eq. (5) switching to conformal time where $d\tau = dt/a$,

$$\partial_\tau \rho_\chi - \frac{n}{\tau} \rho_\chi = -\bar{\sigma} E^2 \frac{1}{\tau}, \quad (7)$$

and we have used $\tau = -1/(aH)$. Taking $\rho_\chi(\tau = \tau_0) = 0$ as the initial condition the solution is,

$$\rho_\chi(\tau) = \frac{\bar{\sigma}}{n} E^2 \left[1 - \left(\frac{\tau_0}{\tau} \right)^{-n} \right]. \quad (8)$$

Note that $\tau_0/\tau_f = e^{N_e}$ with N_e the number of e-folds. So if Schwinger production starts just a few e-folds before the end of inflation, during which the electric field stays constant, then at the end of inflation we will have,

$$\rho_\chi^{\text{end}} \equiv \rho_\chi(\tau_{\text{end}}) \simeq \frac{\bar{\sigma}}{n} E^2 = \frac{\bar{\sigma}}{n} 2\rho_E^{\text{end}}, \quad (9)$$

where the energy density in the dark electric field is given by $\rho_E = \frac{1}{2} E^2$ [13]. We see that at the end of inflation the energy density of the dark charged particles is proportional to the dark electric field energy density, but

³ For these considerations to be sensible, $\langle E \cdot J \rangle$ must be positive, that is $\sigma > 0$. It was pointed out in [23] that the conductivity could turn negative in the limit of weak electric force and small mass of the charged particle. However this effect is unlikely to be physical [24]. We believe this point deserves further investigation which we leave for ongoing work. In this study we assume that the conductivity is always positive.

suppressed by the (dimensionless) conductivity. This result holds for both scalars and fermions and is independent of the source for the dark electric field. The only requirement is that it be (approximately) constant within a Hubble patch and contribute *some* amount to the energy density of the dark vector. Thus any mechanism which generates a constant background dark electric field during inflation will also Schwinger produce some amount of dark particles. If the dark sector does *not* thermalize with itself, the amount of dark charged particles today is determined simply by how much they are produced by the Schwinger effect and redshifting.

In visible QED, after inflation and reheating the Standard Model (SM) plasma thermalizes and erases any initial seed of Schwinger produced electrons as well as any classical electric field generated during inflation. Similar conclusions follow for a dark QED sector which thermalizes with itself [20]. In this work we take the dark gauge coupling to be small enough that the dark QED sector never thermalizes within itself. We will see that for the dark electric field production mechanism considered here, this follows from requiring χ to be non-relativistic by matter radiation equality which imposes an upper bound on g_D (see Eq. (49)). We also assume the dark sector is secluded from the visible one. Thus, any classical dark electric field will persist after reheating and redshift like radiation, all the while continuing to pair produce dark charged particles via the Schwinger mechanism.

After reheating, which we assume to be instantaneous for simplicity, we can write Eq. (5) as,

$$\dot{\rho}_\chi + nH(t)\rho_\chi = \sigma(t)2\rho_E(t), \quad (10)$$

where we parametrize how various quantities redshift as,

$$\begin{aligned} H(t) &= H_{\text{RH}} \left(\frac{T}{T_{\text{RH}}} \right)^\delta, \\ \sigma(t) &= \sigma_{\text{end}} \left(\frac{a_{\text{end}}}{a} \right)^\alpha = \sigma_{\text{RH}} \left(\frac{T}{T_{\text{RH}}} \right)^\alpha, \\ \rho_E(t) &= \rho_E^{\text{end}} \left(\frac{a_{\text{end}}}{a} \right)^4 = \rho_E^{\text{RH}} \left(\frac{T}{T_{\text{RH}}} \right)^4, \end{aligned} \quad (11)$$

where RH refers to quantities defined at the end of reheating. In radiation domination one has $\delta = 2$, but we keep it unspecified for now to allow for other possibilities ($\delta = 3/2$ for matter domination for instance). It is unknown how the conductivity evolves after reheating as it requires calculation of the Schwinger current in an FRW background. Regardless, it is reasonable to assume it will not increase given that the electric field decreases due to redshifting. We thus expect σ either to remain constant or to redshift at some rate. We parametrize this ignorance with the power scaling parameter $\alpha \geq 0$.

It is convenient to rewrite Eq. (10) switching variables

from cosmic time t to temperature T ,

$$\frac{d\rho_\chi}{dT} - \frac{n}{T}\rho_\chi = -2\bar{\sigma}_{\text{RH}} \frac{\rho_E^{\text{RH}}}{T_{\text{RH}}} \left(\frac{T}{T_{\text{RH}}} \right)^{3+\alpha-\delta}, \quad (12)$$

where $\bar{\sigma}_{\text{RH}} \equiv \sigma_{\text{RH}}/H_{\text{RH}}$. We take as the initial boundary condition at the end of reheating the amount of energy density produced at the end of inflation from Eq. (9),

$$\rho_\chi(T_{\text{RH}}) \equiv \rho_\chi^{\text{RH}} = \rho_\chi^{\text{end}} = \frac{\bar{\sigma}_{\text{end}}}{n} 2\rho_E^{\text{end}} = \frac{\bar{\sigma}_{\text{RH}}}{n} 2\rho_E^{\text{RH}}. \quad (13)$$

Then general the solution to Eq. (12) is given by,

$$\rho_\chi(T) = \frac{2\bar{\sigma}_{\text{RH}}\rho_E^{\text{RH}}}{n-4-\alpha+\delta} \left[\left(\frac{T}{T_{\text{RH}}} \right)^{4+\alpha-\delta} - \frac{(4+\alpha-\delta)}{n} \left(\frac{T}{T_{\text{RH}}} \right)^n \right]. \quad (14)$$

To gain some intuition, consider the case in which the produced χ particles are relativistic, the universe is radiation dominated (visible sector radiation), and the conductivity does not redshift which gives,

$$n = 4, \quad \delta = 2, \quad \alpha = 0. \quad (15)$$

Then Eq. (15) becomes,

$$\begin{aligned} \rho_\chi(T) &= \bar{\sigma}_{\text{RH}}\rho_E^{\text{RH}} \left[\left(\frac{T}{T_{\text{RH}}} \right)^2 - \frac{1}{2} \left(\frac{T}{T_{\text{RH}}} \right)^4 \right] \\ &\simeq \bar{\sigma}_{\text{RH}}\rho_E^{\text{RH}} \left(\frac{T}{T_{\text{RH}}} \right)^2, \end{aligned} \quad (16)$$

where in the last equality we neglect the T^4 term compared to T^2 as it becomes less important as the universe expands and the temperature decreases. In the absence of Schwinger production χ would redshift like radiation as $\propto T^4$ after reheating. However, the persistence of the dark electric field and of Schwinger production contributes to ρ_χ thus making it redshift slower as $\propto T^2$.

Generating dark electric fields during inflation

In order to form a classical dark electric field which can source Schwinger production during and after inflation, the vector bosons must be produced in a configuration with a very large occupation number and a coherence wavelength atleast of order the horizon, H^{-1} . Here we describe how to generate such a dark electric field during inflation. Mechanisms for producing a vector field during inflation can be constructed in a number of ways. One possibility is to consider a minimal coupling to the metric via a vector mass term [2, 10]. Alternatively, one can consider non-minimal couplings between the inflaton and the gauge field. The two most common such couplings are ones between (a function of the) the inflaton and the

kinetic term of the gauge field $I(\phi)FF$ [9, 33, 34] or the dual field strength $I(\phi)F\tilde{F}$ [6, 13, 35].

Motivated by, but not limited to models of axion inflation [36], here we focus on the mechanism presented in [6, 13] which produces only *one transverse* mode of the dark vector field and works even if the dark vector is massless. This mechanism utilizes the $\phi F\tilde{F}$ operator which introduces a source of conformal symmetry violation and a time dependence into the dark vector dispersion relation. This induces a tachyonic instability and leads to exponential production (very high occupation number) of one of the transverse modes with a coherence length $l \gtrsim H_{\text{end}}^{-1}$ [6, 13]. Thus we have a (approximately) constant classical electric field within each Hubble patch which can serve as the source for Schwinger production.

We add to the action in Eq. (1) the Lagrangian,

$$\mathcal{L}_{\text{source}}(A_\mu, \phi) = -\frac{1}{2}\partial_\mu\phi\partial^\mu\phi - V(\phi) - \frac{\alpha}{4f}\phi F_{\mu\nu}\tilde{F}^{\mu\nu}, \quad (17)$$

where ϕ is the inflaton field that drives inflation and $\tilde{F}^{\mu\nu} = \epsilon^{\mu\nu\alpha\beta}F_{\alpha\beta}/2$ with $\epsilon^{\mu\nu\alpha\beta}$ the completely antisymmetric tensor. We do not specify the inflaton potential $V(\phi)$ as its precise form is not crucial for the production mechanism considered here, but can affect the shape of the energy density spectrum as explored in detail in [13]. The dark vector can in principle have a mass, as long as it is small compared to the Hubble scale at the end of inflation. We neglect the vector mass for the rest of this section, but we will consider it when examining the evolution of the energy densities after reheating.

The coupling $\alpha/(4f)$ introduces the scale f and a source of conformal symmetry breaking into the theory which leads to the production of a large number of dark photons at the expense of the kinetic energy of the inflaton [37, 38]. We consider a regime where $\alpha/(4f)$ is small enough to ignore the back reaction effects on the inflaton due to dark photon production. In doing so, we only need to write the equation of motion for A_μ . In the presence of dark charged particles, or equivalently of non-zero conductivity, the equation of motion is,

$$\ddot{A}_\pm + H(1 + \bar{\sigma})\dot{A}_\pm + \left(\frac{k^2}{a^2} \mp 2\xi H \frac{k}{a}\right)A_\pm = 0, \quad (18)$$

where \pm refers to the helicities of the transverse modes and we have defined the ‘instability parameter’,

$$\xi \equiv \frac{\alpha\dot{\phi}}{2Hf} = \sqrt{\frac{\epsilon}{2}}\frac{\alpha}{f}M_{\text{Pl}}. \quad (19)$$

The ‘slow roll’ parameter is defined as $\epsilon \equiv -\dot{H}/H^2$ where in single field inflation we have the relations,

$$|\dot{\phi}| \approx V'/3H, \quad \epsilon = \frac{\dot{\phi}^2}{2H^2M_{\text{Pl}}^2}. \quad (20)$$

Note the conductivity enters as a correction to the Hubble damping term in Eq. (18). As stated in Eq. (6), we

work in the regime $\bar{\sigma} \ll 1$, so we can neglect the effect of the conductivity on the transverse vector mode equation of motion. Taking ξ to be time-independent, the solution can be found in terms of Whittaker functions using the WKB approximation as shown in [13] for instance, to which we refer the reader for details. From Eq. (18) we see that when $k/a \lesssim 2\xi H$, one of the transverse modes becomes tachyonic (which we take to be A_+) and exponentially enhanced (large occupation number) which we can associate with particle production of the dark vector [6, 13]. In our regime of interest, where we can neglect backreaction effects while still generating enough particle production, ξ typically takes values between 1 and 9 at the end of inflation. Thus exponential particle production occurs when the wavelength of the dark vector is comparable to the size of the horizon. This generates a classical background dark electric field with a coherence length of order the inverse Hubble scale. This dark electric field can then act as a source for Schwinger pair production during and after inflation.

To estimate how large the dark electric field is we can compute the energy density contained in the electric field. Since the parameter ξ increases with time, as $\dot{\phi}$ increases and H decreases, it is largest at the end of inflation and in principle depends on time. In [13] the effect of this time dependence was taken into account in numerical solutions of Eq. (18) and shown that, while the time dependence can effect the shape and peak of the energy density power spectrum, the *average* energy density is sufficiently well approximated using analytic solutions to obtain order of magnitude estimates of the dark matter parameter space. Using the WKB approximation to solve Eq. (18) one finds [6, 13],

$$\begin{aligned} \rho_E &\equiv \langle \rho_E \rangle = \frac{1}{2} \langle |E_+|^2 \rangle = \frac{1}{2} \langle \frac{1}{a^2} |\partial_t A_+|^2 \rangle \\ &\approx 10^{-4} \frac{e^{2\pi\xi}}{\xi^3} H^4. \end{aligned} \quad (21)$$

Here $\rho_E \equiv \langle \rho_E \rangle$ represents the spacial average of the total dark electric field energy density, where most of the energy is stored as the one in the dark magnetic field is suppressed by $\rho_B = \rho_E/\xi^2$. As shown in [13], this result is in decent agreement with the numerical result which takes into account the time variation of ξ . Taking ξ and H constant, we see from Eq. (21) that the magnitude of the physical dark electric field sourced by the rolling inflaton remains constant. This is a reasonable approximation when we are close to the end of inflation as ξ and Hubble change little in the last few e-folds. Since the energy density is exponentially sensitive to ξ which increases towards the end of inflation, as the slow roll parameter increases, the vast majority of the dark electric field is produced at the end of inflation. Hence, in the last few e-folds of inflation we obtain a roughly constant dark electric field of order the Hubble horizon and we can

apply Eq. (8) and Eq. (9) to compute the energy density of the Schwinger produced dark charged particles.

To produce particles during inflation it is in general necessary to break conformal invariance. We emphasize that here we consider a single source of conformal breaking generated by the axion like coupling between the inflaton and the dark photon, α/f in Eq. (17) which introduces a new scale. As discussed above, we take the dark charged particles χ to be conformally coupled by neglecting their mass during inflation, $m_\chi \ll H$ (and by taking $\xi_R = 1/6$ in Eq. (2) for the scalar case). This ensures there is no purely gravitational particle production [30, 31] and we can isolate the the particle production due to the inflationary Schwinger effect.

Conductivity and weak electric force regime

So far we have used the conductivity σ to parametrize and quantify the energy density of the particles produced via the Schwinger effect. Such an effect in flat spacetime depends on the “electric force” ($g_D E$) as well as on the mass of the charged particle and leads to an exponential suppression $\propto \exp[-m_\chi^2/|g_D E|]$. In de-Sitter space expansion introduces one more parameter in the Hubble scale H and non exponentially suppressed regimes become possible. In this section we give a brief account of how the conductivity is expected to behave in the regime we are interested in. For this we rely on previous studies of the Schwinger effect in a de-Sitter background [22–24].

The strong electric force regime where $g_D E > H^2$ was studied in [32] which showed that this condition also implies $m_\chi > H$. In this regime dark Schwinger production dominates over the exponentially suppressed (with m_χ/H) contribution arising from purely gravitational effects. Furthermore, the Schwinger effect exhibits the same behaviour in de-Sitter space as in flat space [22, 24]. However, in the weak force regime, no Schwinger production occurs in flat space while in de-Sitter space it can still occur and exhibits various non-intuitive features [23, 24]. Here we examine whether dark Schwinger production can also generate enough dark matter in the weak electric force regime where,

$$|g_D E| \ll H^2. \quad (22)$$

As discussed above, in order to ensure it is not dominated by (purely) gravitational effects [30, 31], we must also be in the conformal limit where $m_\chi/H_{\text{end}} \ll 1$ during inflation. (and $\xi_R = 1/6$ for the scalar case).

As our dark electric field has a magnitude typically much larger than H^2 , given the exponential enhancement in Eq. (21), we must have a weak gauge coupling,

$$g_D \ll \frac{H^2}{E} = 10^2 \frac{\xi^{3/2}}{e^{\pi\xi}}. \quad (23)$$

To see how the conductivity is related to the gauge coupling let us consider the case of scalar dark charged particles [22, 24]. In the weak electric force regime the conductivity is given by [22],

$$\sigma = g_D^2 \frac{H}{24\pi^2} \left[\ln \left(\frac{\xi_R R}{H^2} \right) + \frac{16\pi}{3} \frac{\mu_0(-1 + \mu_0^2)}{\sin(2\pi\mu_0)} - \psi \left(\frac{1}{2} + \mu_0 \right) - \psi \left(\frac{1}{2} - \mu_0 \right) \right], \quad (24)$$

where we have defined,

$$\mu_0^2 = \frac{9}{4} - \frac{\xi_R R}{H^2}, \quad (25)$$

with ψ the digamma function and we have taken $m_\chi = 0$ in Eq. (2). Setting $\xi_R = 1/6$ for the conformally coupled scalar and recalling that $R = 12H^2$ in de-Sitter gives,

$$\bar{\sigma} = \frac{\sigma}{H} = \frac{g_D^2}{24\pi^2} \left[\ln 2 + \frac{2}{3} + 2\gamma_E \right] \approx 10^{-2} g_D^2, \quad (26)$$

where γ_E is the Euler gamma constant. Note we find a similar order of magnitude estimate for the fermion case as well [23]. We see that the conductivity is $\propto g_D^2$ so a small gauge coupling $g_D \ll 1$ guarantees a small σ in this case. In the next section we will see that the cosmic evolution imposes bounds on g_D stronger than Eq. (23).

COSMIC EVOLUTION AND DARK SECTOR RELIC ABUNDANCE

At the end of inflation the inflaton still dominates the energy density of the Universe with,

$$\rho_I^{\text{end}} = 3H_{\text{end}}^2 M_{\text{Pl}}^2. \quad (27)$$

A small part of this initial energy density is transferred to the dark photon. As discussed above, this energy is mostly stored in the classical dark electric field (see Eq. (21)) with energy density at the end of inflation,

$$\rho_E^{\text{end}} \equiv \rho_A(T_{\text{RH}}) \approx 10^{-4} \frac{e^{2\pi\xi_{\text{end}}}}{\xi_{\text{end}}^3} H_{\text{end}}^4. \quad (28)$$

A small fraction of ρ_E^{end} then goes into pair producing χ via the dark Schwinger mechanism,

$$\rho_\chi^{\text{end}} = \frac{2\bar{\sigma}_{\text{end}}}{n} \rho_E^{\text{end}}. \quad (29)$$

The fraction of ρ_I^{end} which goes into visible radiation to reheat the universe, a process that we consider instantaneous here for simplicity, is parametrized by the dimensionless quantity ϵ_R defined by,

$$\rho_R(T_{\text{RH}}) = \frac{\pi^2}{30} g_*(T_{\text{RH}}) T_{\text{RH}}^4 \equiv \epsilon_R^4 \rho_I^{\text{end}} = 3H_{\text{RH}}^2 M_{\text{Pl}}^2. \quad (30)$$

Here $g_*(T_{\text{RH}})$ denotes the number of relativistic degrees of freedom which we fix to $g_*(T_{\text{RH}}) \sim 100$, restricting ourselves to reheating temperatures above the electroweak scale. We see Eq. (30) also defines the relation between the value of Hubble at reheating H_{RH} , which we introduced in Eq. (11), and H_{end} at the end of inflation,

$$H_{\text{RH}} = \epsilon_R^2 H_{\text{end}}. \quad (31)$$

At reheating the dark vector and χ have energy densities,

$$\rho_A(T_{\text{RH}}) \equiv \rho_E^{\text{RH}} = \rho_E^{\text{end}}, \quad (32)$$

$$\rho_\chi^{\text{RH}} = \rho_\chi^{\text{end}}, \quad (33)$$

with the following hierarchies,

$$\rho_\chi^{\text{RH}} \ll \rho_A(T_{\text{RH}}) \ll \rho_R(T_{\text{RH}}) \ll \rho_I^{\text{end}}. \quad (34)$$

We assume that the dark and visible sectors are decoupled and that the dark sector does not thermalize with itself. While at reheating ρ_χ starts as the smallest energy density, it grows during the radiation domination era due to continued Schwinger production (see Eq. (15)). Furthermore, when the momentum redshifts below m_χ , at which point Schwinger production becomes highly suppressed, the energy density in χ will begin to redshift like matter as a^{-3} and eventually becomes dominant after matter radiation equality. For the mechanism considered here, the dark vector can be massless, in which case its energy density continues redshifting like radiation and remains negligibly subdominant throughout its cosmic evolution. In what follows however, we consider a massive vector, in which case it eventually becomes non-relativistic and contributes to the dark matter abundance also. The massless case is recovered by setting $m_A = 0$.

Let us now track the evolution of the energy densities, starting with the vector. As shown in [6, 13], for a given scale factor, the power spectrum of the dark vector will be peaked around scales the size of the horizon. Thus, the modes which give the largest contribution to ρ_A at reheating have physical momentum,

$$q_A(T_{\text{RH}}) \equiv \frac{k}{a_{\text{RH}}} = \frac{k}{a_{\text{end}}} \simeq H_{\text{end}} \gg m_A. \quad (35)$$

As the universe expands and the temperature decreases the momentum redshifts as,

$$q_A(T) = \frac{T}{T_{\text{RH}}} H_{\text{end}}. \quad (36)$$

The dark photons then become non-relativistic when $q_A(\bar{T}_A) = m_A$ which occurs at the temperature,

$$\bar{T}_A = \frac{m_A}{H_{\text{end}}} T_{\text{RH}}. \quad (37)$$

Above \bar{T}_A their energy density redshifts like radiation,

$$\rho_A(T) = \rho_A(T_{\text{RH}}) \left(\frac{T}{T_{\text{RH}}} \right)^4, \quad (38)$$

while below \bar{T}_A it redshifts like matter giving,

$$\rho_A(T) = \rho_A(T_0) \left(\frac{T}{T_0} \right)^3, \quad (39)$$

where $T_0 \approx 10^{-13}$ GeV is today's CMB temperature. From this we obtain the energy density today [6, 13],

$$\rho_A(T_0) = \left(\frac{T_0}{T_{\text{RH}}} \right)^3 \left(\frac{m_A}{H_{\text{end}}} \right) \rho_A(T_{\text{RH}}). \quad (40)$$

As shown in [6, 13], the dark vector can account for the entirety of the dark matter over a very large range of dark vector masses $\sim \mu\text{eV} - 10\text{TeV}$. Furthermore, due to large density fluctuations, today the vector dark matter has a clumpy like nature on physical scales $\sim cm - 100\text{km}$ [13].

Next we turn to the evolution of ρ_χ . After reheating the energy density of χ evolves as described by Eq. (15), with $n = 4$ (relativistic) and $\delta = 2$ (radiation),

$$\rho_\chi(T) = \frac{2\bar{\sigma}_{\text{RH}}\rho_E^{\text{RH}}}{2-\alpha} \left[\left(\frac{T}{T_{\text{RH}}} \right)^{2+\alpha} - \frac{(2+\alpha)}{4} \left(\frac{T}{T_{\text{RH}}} \right)^4 \right]. \quad (41)$$

Here α parametrizes the possible redshift scaling of the conductivity $\sigma = \sigma_{\text{RH}}(T/T_{\text{RH}})^\alpha$ as defined in Eq. (11)). If $0 \leq \alpha < 2$ the first term in Eq. (41) dominates as T decreases and $\rho_\chi(T)$ redshifts slower than radiation. The case $\alpha = 2$ corresponds to the conductivity redshifting like Hubble and results in,

$$\rho_\chi(T) = \frac{\bar{\sigma}_{\text{RH}}\rho_E^{\text{RH}}}{2} \left(\frac{T}{T_{\text{RH}}} \right)^4 \left[1 - \ln \left(\frac{T}{T_{\text{RH}}} \right)^4 \right]. \quad (42)$$

Thus it redshifts almost like radiation apart from a logarithmic correction. If $\alpha > 2$ the last term in Eq. (41) dominates and the redshift is like radiation. We see that only if the conductivity redshifts slower than Hubble do we have a significant contribution to ρ_χ during radiation domination. Thus, if $\alpha \geq 2$ we can neglect Schwinger production after reheating and just follow the evolution of ρ_χ that was produced during inflation.

The next step is to determine when χ becomes non-relativistic which requires tracking its momentum. During inflation χ is produced at the (negligible) expense of the energy density of the dark electric field. As ρ_E peaks at a wavelength the size of the horizon, it is reasonable to expect that χ inherits a power spectrum peaked at the same wavelength. Thus, the typical momentum of χ at reheating is the same as that of the vector,

$$q_\chi(T_{\text{RH}}) \simeq H_{\text{end}} \gg m_\chi. \quad (43)$$

This evolves in time according to,

$$\frac{dq_\chi}{dt} + Hq_\chi = g_D E(t). \quad (44)$$

The momentum redshifts due to the expansion of the universe, but at the same time it tends to increase due to

the dark electric force accelerating χ . The physical dark electric field $E(t)$ decreases in time. Again we switch to temperature to track the evolution which gives,

$$E(T) = \sqrt{2\rho_E(T)} = \sqrt{2\rho_E^{\text{RH}}} \left(\frac{T}{T_{\text{RH}}} \right)^2, \quad (45)$$

and Eq. (44) becomes,

$$\frac{dq_\chi}{dT} - \frac{q_\chi}{T} = -\frac{g_D}{T} \frac{\sqrt{2\rho_E^{\text{RH}}}}{H_{\text{RH}}}, \quad (46)$$

which has a solution of the form,

$$q_\chi(T) = q_\chi(T_{\text{RH}}) \frac{T}{T_{\text{RH}}} + g_D \frac{\sqrt{2\rho_E^{\text{RH}}}}{H_{\text{RH}}} \left(1 - \frac{T}{T_{\text{RH}}} \right). \quad (47)$$

The momentum must decrease with decreasing temperature if χ is to become non-relativistic. This implies a maximum dark gauge coupling $g_D < H_{\text{end}} H_{\text{RH}} / \sqrt{2\rho_E^{\text{RH}}}$ and reflects the fact that the gauge coupling must be weak enough to ensure that momentum redshifting dominates over the effect of the acceleration due to the dark electric field. However, there are more stringent bounds on the gauge coupling coming from requiring χ to become non-relativistic by the time of matter radiation equality (MRE) at temperature $T_{\text{MRE}} \sim \text{eV}$. We can solve for the temperature at which χ becomes non-relativistic using $q_\chi(\bar{T}_\chi) = m_\chi$ and Eq. (47) which gives,

$$\bar{T}_\chi = \frac{H_{\text{RH}} m_\chi - g_D \sqrt{2\rho_E^{\text{RH}}}}{H_{\text{end}} H_{\text{RH}} - g_D \sqrt{2\rho_E^{\text{RH}}}} T_{\text{RH}}. \quad (48)$$

Thus, we have the condition $T_{\text{MRE}} < \bar{T}_\chi < T_{\text{RH}}$ which translates into the bound on the gauge coupling

$$\begin{aligned} g_D &< \frac{\epsilon_R^2 H_{\text{end}}^2}{E} \left(\frac{m_\chi}{H_{\text{end}}} - \frac{T_{\text{MRE}}}{T_{\text{RH}}} \right) \\ &= 50\sqrt{2} \frac{\xi_{\text{end}}^{3/2}}{e\pi\xi_{\text{end}}} \epsilon_R^2 \left(\frac{m_\chi}{H_{\text{end}}} - \frac{T_{\text{MRE}}}{T_{\text{RH}}} \right), \end{aligned} \quad (49)$$

together with the condition,

$$\frac{T_{\text{MRE}}}{T_{\text{RH}}} < \frac{m_\chi}{H_{\text{end}}} \ll 1, \quad (50)$$

to keep g_D positive which will be the case over all of the parameter space we consider. In fact Eq. (49) also holds when $m_\chi > H_{\text{end}}$, but since we are working in the conformal limit we limit ourselves to $m_\chi < H_{\text{end}}$. Note that Eq. (49) gives a much stronger upper bound on g_D compared to Eq. (23), due to the further suppression proportional to $\epsilon_R^2 (m_\chi/H_{\text{end}})$. The bound in Eq. (49) can push the gauge coupling to very small values in some regions

of parameter space and we restrict ourselves to the region in which we satisfy the weak gravity conjecture [39],

$$g_D > \frac{m_\chi}{M_{\text{Pl}}}. \quad (51)$$

Above \bar{T}_χ the energy density of χ evolves according to Eq. (41). When χ becomes non-relativistic the Schwinger production is no longer effective. We must also ensure that $\rho_\chi(\bar{T}_\chi) \ll \rho_A(\bar{T}_\chi)$ is satisfied all the way down to \bar{T}_χ in order to justify neglecting the back reaction of the Schwinger production on the dark electric field as we have assumed in our analysis. This is always ensured when g_D satisfies Eq. (49) so our analysis is self consistent. Below \bar{T}_χ the charged particles redshift like matter,

$$\rho_\chi(T) = \rho_\chi(T_0) \left(\frac{T}{T_0} \right)^3, \quad (52)$$

analogously to Eq. (39). The energy density today is found by equating Eq. (41) and Eq. (52) at $T = \bar{T}_\chi$,

$$\begin{aligned} \rho_\chi(T_0) &= \frac{1}{2} \bar{\sigma}_{\text{RH}} \rho_E^{\text{RH}} \left(\frac{T_0}{T_{\text{RH}}} \right)^3 \\ &\times \frac{1}{2-\alpha} \left[4 \left(\frac{m_\chi}{H_{\text{end}}} \right)^{\alpha-1} - (2+\alpha) \left(\frac{m_\chi}{H_{\text{end}}} \right) \right], \end{aligned} \quad (53)$$

where we have expanded in powers of the small dark gauge coupling keeping only the leading order term and recalling that $\bar{\sigma}_{\text{RH}} \propto g_D^2$ (see Eq. (26)). This result has several interesting features. If the conductivity remains constant after reheating ($\alpha = 0$) the final relic density ρ_χ gets enhanced by $H_{\text{end}}/m_\chi \gg 1$,

$$\rho_\chi(T_0) \simeq \bar{\sigma}_{\text{RH}} \rho_E^{\text{RH}} \left(\frac{T_0}{T_{\text{RH}}} \right)^3 \frac{H_{\text{end}}}{m_\chi} \quad (\alpha = 0). \quad (54)$$

Note in this expression H_{end}/m_χ cannot be arbitrarily large because it is bound by Eq. (50). An enhancement of $(H_{\text{end}}/m_\chi)^{1-\alpha}$ persists as long as the conductivity redshifts slowly enough ($0 \leq \alpha < 1$). When $\alpha = 1$ we reach a value independent of m_χ to a good approximation,

$$\rho_\chi(T_0) \simeq 2\bar{\sigma}_{\text{RH}} \rho_E^{\text{RH}} \left(\frac{T_0}{T_{\text{RH}}} \right)^3 \quad (\alpha = 1). \quad (55)$$

For values $1 < \alpha < 2$, the final relic abundance is suppressed by $(m_\chi/H_{\text{end}})^{\alpha-1}$. When the conductivity redshifts like Hubble ($\alpha = 2$) in radiation domination,

$$\begin{aligned} \rho_\chi(T_0) &= \frac{1}{2} \bar{\sigma}_{\text{RH}} \rho_E^{\text{RH}} \left(\frac{T_0}{T_{\text{RH}}} \right)^3 \\ &\times \frac{m_\chi}{H_{\text{end}}} \left[1 - \ln \left(\frac{m_\chi}{H_{\text{end}}} \right)^4 \right] \quad (\alpha = 2). \end{aligned} \quad (56)$$

When the conductivity redshifts faster ($\alpha \gg 2$) this gives,

$$\rho_\chi(T_0) = \frac{1}{2} \bar{\sigma}_{\text{RH}} \rho_E^{\text{RH}} \left(\frac{T_0}{T_{\text{RH}}} \right)^3 \frac{m_\chi}{H_{\text{end}}} \quad (\alpha \gg 2). \quad (57)$$

In this last case the contribution to ρ_χ comes entirely from the Schwinger production at the end of inflation with the production after reheating being negligible.

The analysis presented is sensible only if the dark sector does not thermalize. Thermalization with the visible sector is easily avoided by taking the dark sector to be secluded. This implies that a possible kinetic mixing between visible and dark $U(1)$ has to be small. We also need to ensure that the dark sector does not thermalize within itself either. This requires that the rate of interactions between the dark charged particles and the dark photon is always slower than Hubble which we can estimate as follows. As long as χ is relativistic its number density is given by $n_\chi(T) \simeq \rho_\chi(T)/q_\chi(T)$ and the two-to-two cross section, mediated by the exchange of a dark photon, can be estimated as $\sigma_{2\rightarrow 2} \sim g_D^4/q_\chi(T)^2$. Here, $\rho_\chi(T)$ and $q_\chi(T)$ are given by Eq. (41) and Eq. (47) respectively. The scattering rate is $\Gamma = n_\chi(T)\sigma_{2\rightarrow 2}$ and is found to have two terms at leading order in g_D , one which scales like T and the other like $T^{\alpha-1}$. So Γ decreases more slowly than $H \propto T^2$ when χ is relativistic. The trend changes when χ becomes non-relativistic at which point Γ scales like T^3 . Hence, we must require that g_D is small enough that $\Gamma < H$ is satisfied all the way down to the temperature \bar{T}_χ . This amounts to the condition,

$$g_D < 10 \times 2^{1/6} \frac{\xi^{1/2}}{e^{\pi\xi/3} \epsilon_R^{1/3}} (2-\alpha)^{1/6} \sqrt{\frac{m_\chi}{H_{\text{end}}}} \times \left[4 \left(\frac{m_\chi}{H_{\text{end}}} \right)^\alpha - (2+\alpha) \left(\frac{m_\chi}{H_{\text{end}}} \right)^2 \right]^{-1/6}. \quad (58)$$

As can be seen, this is a weaker bound for any α compared to Eq. (49) which follows from requiring χ is non-relativistic by matter radiation equality. Thus, we are guaranteed that the dark sector does not thermalize in the mechanism proposed in this study.

With the various energy densities today in hand we can examine the parameter space in which the observed dark matter relic abundance is reproduced. Taking the observed energy density of cold dark matter today [40] to be $\rho_{\text{CDM}} = 9.6 \times 10^{-48} \text{ GeV}^4$, the contribution from the dark vector is given by [6, 13],

$$\frac{\Omega_A}{\Omega_{\text{CDM}}} = \frac{\rho_A(T_0)}{\rho_{\text{CDM}}} \simeq 0.2 \times \left(\frac{m_A}{\text{GeV}} \right) \left(\frac{H_{\text{end}}}{10^{14} \text{ GeV}} \right)^{3/2} \frac{e^{2\pi\xi_{\text{end}}}}{\epsilon_R^3 \xi_{\text{end}}^3}. \quad (59)$$

The contribution from the dark charged particles is,

$$\frac{\Omega_\chi}{\Omega_{\text{CDM}}} = \frac{\rho_\chi(T_0)}{\rho_{\text{CDM}}} \simeq 10^{10} \bar{\sigma}_{\text{RH}} \left(\frac{H_{\text{end}}}{10^{14} \text{ GeV}} \right)^{5/2} \frac{e^{2\pi\xi_{\text{end}}}}{\epsilon_R^3 \xi_{\text{end}}^3} \times \frac{1}{2-\alpha} \left[4 \left(\frac{m_\chi}{H_{\text{end}}} \right)^{\alpha-1} - (2+\alpha) \left(\frac{m_\chi}{H_{\text{end}}} \right) \right]. \quad (60)$$

This is proportional to the value of the conductivity at reheating which is the same as at the end of inflation and proportional to g_D^2 (see Eq. (26)). Clearly, if we switch off the gauge interactions in the dark sector we turn off the dark Schwinger production and we have no relics in the form of dark charged particles. To arrive at Eq. (60) we assumed that the conductivity redshifts as $a^{-\alpha}$ during the radiation dominated era (see Eq. (11)) giving,

$$\bar{\sigma}(T) = \bar{\sigma}_{\text{RH}} \left(\frac{T}{T_{\text{RH}}} \right)^\alpha \simeq 10^{-2} g_D^2 \left(\frac{T}{T_{\text{RH}}} \right)^\alpha. \quad (61)$$

In the last equality we used Eq. (26) as an estimate for the relation between the conductivity and the gauge coupling. This holds approximately for both dark charged fermions and scalars [22–24] and will be useful to explore the relic density parameter space as a function of g_D . In principle, we can have a mixture of dark vector and dark scalars/fermions as dark matter. The case in which Ω_A dominates reduces to what was studied in [6, 13]. Here we focus on the case in which Ω_χ dominates. In particular, as discussed previously, the mechanism proposed here is also viable when the dark photon is massless in which case Ω_A is negligible and the dark matter is composed entirely of Schwinger produced dark charged particles.

Dark matter parameter space

Having followed the cosmic evolution of the dark sector energy density and found an estimate for the relic abundance today, we can go on to estimate the regions of parameter space for a viable dark matter sector. To find these regions, we must ensure that not only the observed cold dark matter relic abundance is reproduced, but also that a number of constraints on the model parameters are satisfied for consistency of the mechanism. To be generic, we briefly summarize the constraints both for the dark photon [6, 13] and for the dark scalar/fermion.

The first constraint is an upper bound on the dark vector mass which results from requiring $m_A < H_{\text{end}}$ for efficient tachyonic production during inflation. If a particular species dominates the dark matter relic abundance then its mass is bounded below by the condition that it becomes non-relativistic, thus behaving like cold dark matter, before matter-radiation equality (MRE). There are also robust constraints coming from astrophysical probes which in the case of fermions can lead to a stronger and absolute lower bound of $\mathcal{O}(100 \text{ eV})$ [41, 42]. These lower bounds only apply to the components of the dark matter which contribute sizeably to the relic abundance. Thus we can consider much lighter dark sector particles as long as they only make up a tiny fraction of the dark matter by the time of MRE. We must also require the hierarchy in energy densities at reheating in Eq. (34). Imposing that the visible radiation

has energy density lower than that at the end of inflation ($\rho_R \ll \rho_I^{\text{end}}$) imposes $\epsilon_R < 1$. To ensure the Universe is radiation dominated until MRE requires that $\rho_R > \rho_E^{\text{end}}$ and translates into an upper bound on H_{end} ,

$$H_{\text{end}} < \sqrt{3} \times 10^2 \xi_{\text{end}}^{3/2} e^{-\pi \xi_{\text{end}}} \epsilon_R^2 M_{\text{Pl}}, \quad (62)$$

once we fix ξ_{end} and ϵ_R . Finally, we must satisfy the bound on the gauge coupling in Eq. (49), along with the condition in Eq. (50), for χ to become non-relativistic before MRE. There are other constraints on this mechanism which should be satisfied [6, 13], but they are weaker than the ones discussed here.

We show contours of $\Omega_\chi/\Omega_{\text{CDM}} = 1$ given in Eq. (60) as a function of m_χ vs. H_{end} assuming different scalings ($\alpha = 0, 1, 2, \gg 2$) for how the conductivity redshifts after reheating (see Eq. (11)). The lower contours show the case of $\epsilon_R = 0.75$, with $\xi_{\text{end}} = 1$ (blue solid) and $\xi_{\text{end}} = 9$ (green dashed) while the upper contours are shown for $\epsilon_R = 10^{-4}$ with $\xi_{\text{end}} = 1$ (solid red). We estimate the dimensionless conductivity at reheating by $\bar{\sigma}_{\text{RH}} = g_D^2 10^{-2}$ (see Eq. (26)) where the dark gauge coupling is taken to be the maximum value allowed by the constraint that χ becomes non-relativistic by the time of MRE and which depends on $\xi_{\text{end}}, \epsilon_R, m_\chi$ (see Eq. (49)). Note that once we take g_D to be its maximum value the relic abundance no longer depends explicitly on ξ_{end} . The dark vector, which can even be massless, is taken to be light enough ($m_A \lesssim 10^{-20} \text{ GeV}$) such that it contributes negligibly to the dark sector relic abundance. Thus, in this case the dark matter is composed entirely of Schwinger pair produced particles with (feeble) self interactions mediated by the exchange of ultra light dark photons.

We see this mechanism generically requires the Hubble scale at the end of inflation to be $H_{\text{end}} \gtrsim 10^8 \text{ GeV}$. We can also see that smaller ϵ_R , or lower reheat temperatures, pushes us to larger masses as well as larger H_{end} since we require $m_\chi < H_{\text{end}}$. This is because smaller ϵ_R pushes us to smaller dark gauge couplings (see Eq. (49)) and thus smaller conductivities which requires larger m_χ to compensate for the additional suppression of ρ_χ . For $\xi_{\text{end}} = 1$ and $\epsilon_R = 10^{-4}$ the contours (red solid) are cutoff at $H_{\text{end}} \sim 10^{11} \text{ GeV}$ due to the requirement that $\rho_R > \rho_E^{\text{end}}$ as given by Eq. (62) and which generically rules out smaller values of ϵ_R . The maximum dark gauge coupling allowed by Eq. (49) takes on values in the range $g_D \sim 10^{-15} - 10^{-22}$. The parameter point $\xi_{\text{end}} = 9$ and $\epsilon_R = 10^{-4}$ on the other hand is ruled out by this constraint. For $\xi_{\text{end}} = 1$ and $\epsilon_R = 0.75$ (blue solid) we can consider H_{end} all the way up to the cosmological limit of $H_{\text{end}} \sim 10^{14} \text{ GeV}$ [43, 44]. In this case the maximum allowed dark gauge coupling takes on values in the range $g_D \sim 0.01 - 10^{-15}$. For $\xi_{\text{end}} = 9$ and $\epsilon_R = 0.75$ (dashed green) the requirement that the gauge coupling be larger than that allowed by the weak gravity conjecture limits us to the narrow range $H_{\text{end}} \sim (10^8 - 10^9) \text{ GeV}$ and the dark gauge coupling is fixed to be $g_D \sim 10^{-10}$.

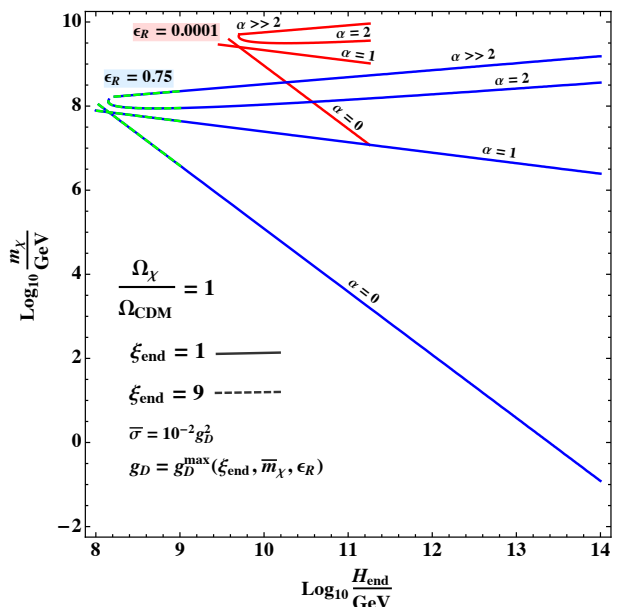


FIG. 1. Contours of $\Omega_\chi/\Omega_{\text{CDM}} = 1$ given in Eq. (60) as a function of m_χ vs. H_{end} assuming $\alpha = 0, 1, 2, \gg 2$ (see Eq. (11)). Above the contour lines we have overabundance, below them underabundance. The lower contours show the case of $\epsilon_R = 0.75$, with $\xi_{\text{end}} = 1$ (blue solid) and $\xi_{\text{end}} = 9$ (green dashed) while the upper contours are shown for $\epsilon_R = 10^{-4}$ with $\xi_{\text{end}} = 1$ (solid red). The dimensionless conductivity is set to $\bar{\sigma}_{\text{RH}} = g_D^2 10^{-2}$ (see Eq. (26)) where g_D is taken to be the maximum value allowed by Eq. (49) which depends on $\xi_{\text{end}}, \epsilon_R, m_\chi$. See text for more information.

We see the observed dark matter relic abundance can be obtained for dark charged particles as light as $m_\chi \sim 10 \text{ MeV}$ for $H_{\text{end}} \sim 10^{14} \text{ GeV}$ and $\xi_{\text{end}} \sim 1$ if the conductivity remains constant after reheating ($\alpha = 0$). In this case Schwinger production takes place almost entirely after inflation. For $\xi_{\text{end}} = 9$ we see we are restricted to the narrow range $m_\chi \sim (10^7 - 10^8) \text{ GeV}$ for Hubble scales at the end of inflation $H_{\text{end}} \sim (10^8 - 10^9) \text{ GeV}$. On the other hand if the conductivity redshifts like Hubble ($\alpha = 2$) or faster then we are restricted to much larger masses in the range $m_\chi \sim (10^8 - 10^{10}) \text{ GeV}$ regardless of the value of ξ_{end} and ϵ_R . In this case, the dark matter is generated almost entirely at the end of inflation.

In summary we can have dark charged particles as the dark matter for masses as light as $\sim 10 \text{ MeV}$ if the conductivity is constant after inflation and as heavy as $m_\chi \sim 10^{10} \text{ GeV}$. This mechanism generically prefers larger Hubble scales at the end of inflation in the range $H_{\text{end}} \sim (10^8 - 10^{14}) \text{ GeV}$. In the end we are left with dark electrons (scalar or fermion) as the dark matter under the influence of a feeble dark QED force mediated by a massless (or very light) dark photon.

We can also examine the parameter space independently of the mechanism for generating the dark elec-

tric field by plotting contours of $\Omega_\chi/\Omega_{\text{CDM}} = 1$ as a function of the ratios $g_D E/H_{\text{end}}^2$ vs. m_χ/H_{end} . We show these contours in Fig. 2 for $\epsilon_R = 0.75$ and only the $\alpha \gg 2$ case where all of the production occurs during inflation and thus is independent of the unknown conductivity after reheating. This also allows for comparison to the parameter space in the strong force [32] regime ($g_D E > H^2$) where the Schwinger production necessarily occurs only during inflation and requires $\epsilon_R \gtrsim 0.5$. We see that while in the strong force regime we are limited to $m_\chi \gtrsim H_{\text{end}} \sim 10^{14} \text{ GeV}$, the weak force case can accommodate Hubble scales down to $H_{\text{end}} \sim 10^8 \text{ GeV}$ and dark matter masses in the range $m_\chi \simeq (10^8 - 10^{10}) \text{ GeV}$. These results hold for any mechanism which can generate a dark electric field during inflation which leads to Schwinger production of dark electron pairs.

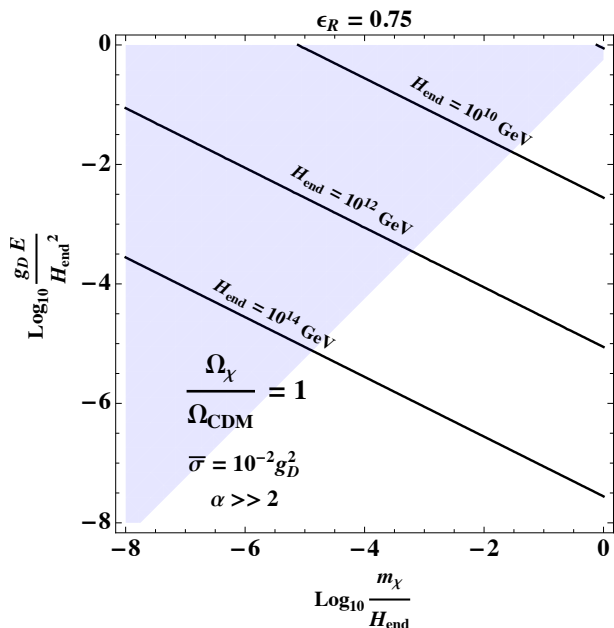


FIG. 2. Contours of $\Omega_\chi/\Omega_{\text{CDM}} = 1$ for $\epsilon_R = 0.75$ and $\alpha \gg 2$ as a function of $g_D E/H_{\text{end}}^2$ vs. m_χ/H_{end} . Above the contour lines we have overabundance, below them underabundance. The light blue region is excluded by the non-relativistic constraint in Eq. (49).

The dark QED sector contained in this mechanism could have a number of interesting phenomenological possibilities. The dark photon could potentially mix with the visible photon leading to a milli-charged dark matter sector with interesting phenomenology [45]. It could also have interesting implications for structure formation as the dark coulomb interaction must be screened at length scales of roughly the size of cluster of galaxies or it would be stronger than the gravitational interaction. Some screening occurs due to the fact that the dark photon will inevitably get an effective mass (plasma frequency) through the interaction with the dark

electron plasma. We can estimate the effective mass at redshift around 100 as $\omega_p(T_*) = g_D \sqrt{\rho_\chi(T_*)}/m_\chi$ taking $T_* \simeq 100 T_0$. This gives $\omega_p(T_*) \sim g_D 10^4 \text{ Mpc}^{-1}$ for $m_\chi \sim 10^{14} \text{ GeV}$ which implies that for a dark gauge coupling $\gtrsim 10^{-4}$ there should be enough screening. We leave a detailed study of the impact of our scenario on structure formation to future work. One should also worry about constraints from the observed triaxiality of dark matter halos [46] and from plasma instabilities [47], but because the dark gauge coupling in the mechanism considered here is so small we should be safe from these bounds. Finally, assisted Schwinger production [48] due to accelerated dark electrons could potentially destroy the dark electric field, but since the dark electrons reach terminal velocity (see Eq. (47)) so quickly we expect this to also have little effect. We leave detailed investigations of these questions to future work.

SUMMARY AND DISCUSSION

We have shown that the observed dark matter relic abundance can be generated via a *dark* Schwinger mechanism which takes place during inflation and/or after reheating. This mechanism leads to a feebly interacting dark sector comprised of dark fermions and/or scalars which can be as light as $\sim 10 \text{ MeV}$ and as heavy as $\sim 10^{10} \text{ GeV}$ depending on how the Schwinger current redshifts after inflation (see Fig. 1). It requires larger Hubble scales at the end of inflation in the range $H_{\text{end}} \sim (10^8 - 10^{14}) \text{ GeV}$ and reheat temperatures which are not too much lower. The necessary background dark electric field is generated during inflation and can in principle continue sourcing Schwinger production of dark charged particles after reheating until they become non-relativistic. The dark matter can exchange ultralight dark photons and has a power spectrum which is peaked at very small scales, thus evading potential isocurvature constraints from measurements of the CMB.

We have discussed possible sources for the constant background dark electric field during inflation with particular focus on the mechanism introduced in [6, 13]. We have derived the energy density of the Schwinger pair produced dark charged particles at the end of inflation (see Eq. (9)) as well as at anytime after reheating (see Eq. (15)). We then derived the relic abundance of the dark sector today (see Eq. (60)) and examined contours where it matches the observed dark matter relic abundance. We have emphasized that in inflationary Schwinger production the background electric field serves as a source of conformal symmetry breaking which is present even in the absence of conformal breaking in the fermion and scalar sectors. Thus even massless fermions or conformally coupled massless scalars, which would not be produced by gravitational particle production due to a changing metric, can still be produced during inflation

(and after) via the inflationary Schwinger effect.

Our analysis relied on analytic calculations of the conductivity associated with the conserved Schwinger current during inflation computed in various studies of inflationary magnetogenesis [23, 24]. The conductivity after reheating has yet to be computed so in this regime we have considered different possibilities for how the conductivity redshifts. Eventually computing the conductivity after inflation will be necessary to make robust predictions and an effort in this direction is ongoing.

Phenomenological implications of the non-thermal dark matter sector considered here depend on how the dark sector communicates with the Standard Model, if at all. For instance a coupling to the Standard Model could occur through kinetic mixing with the photon. Another possibility is through Higgs mixing or through the neutrino sector. Even if the dark sector does not communicate with the Standard Model it could have implications for intermediate scale structure or gravitational waves associated with phase transitions in the dark sector. Furthermore, we can have a multi-component dark sector composed of fermions/scalars exchanging an ultra-light vector which could have interesting effects on dark matter phenomenology. All of these possibilities are potentially interesting and deserve further investigation.

Acknowledgments: The authors thank Antonio Torres Manso, Manel Masip, Jose Santiago and Takeshi Kobayashi for useful comments and discussions. This work has been partially supported by Junta de Andalucía Project A-FQM-472-UGR20 (fondos FEDER) (R.V.M.) and by SRA (10.13039/501100011033) and ERDF under grant PID2022-139466NB-C21(R.V.M.) as well as by MICINN (PID2019-105943GB-I00/AEI/10.13039/501100011033,PID2022.140831NB.I00/AEI/10.13039/501100011033/FEDER,UE) (M.B.G.), FCT-CERN grant No. CERN/FIS-PAR/0027/2021 (M.B.G., P.F.), FCT Grant No.SFRH/BD/151475/2021 (P.F.). The work of LU was supported by the Slovenian Research Agency under the research core funding No. P1-0035 and in part by the research grant J1-4389. This article is based upon work from COST Action COSMIC WISPerS CA21106, supported by COST (European Cooperation in Science and Technology).

* mbg@ugr.es

† paulo.ferraz@student.uc.pt

‡ lorenzo.ubaldi@ijs.si

§ rvegamos@ugr.es

[1] G. Bertone and M. P. Tait, *Tim*, **Nature** **562**, 51 (2018), 1810.01668.
 [2] P. W. Graham, J. Mardon, and S. Rajendran, *Phys. Rev.*

D93, 103520 (2016), 1504.02102.
 [3] P. Agrawal, N. Kitajima, M. Reece, T. Sekiguchi, and F. Takahashi, *Phys. Lett.* **B801**, 135136 (2020), 1810.07188.
 [4] J. A. Dror, K. Harigaya, and V. Narayan, *Phys. Rev.* **D99**, 035036 (2019), 1810.07195.
 [5] R. T. Co, A. Pierce, Z. Zhang, and Y. Zhao, *Phys. Rev.* **D99**, 075002 (2019), 1810.07196.
 [6] M. Bastero-Gil, J. Santiago, L. Ubaldi, and R. Vega-Morales, *JCAP* **1904**, 015 (2019), 1810.07208.
 [7] A. J. Long and L.-T. Wang, *Phys. Rev. D* **99**, 063529 (2019), 1901.03312.
 [8] S. D. McDermott and S. J. Witte, *Phys. Rev. D* **101**, 063030 (2020), 1911.05086.
 [9] Y. Nakai, R. Namba, and Z. Wang (2020), 2004.10743.
 [10] A. Ahmed, B. Grzadkowski, and A. Socha, *JHEP* **08**, 059 (2020), 2005.01766.
 [11] E. W. Kolb and A. J. Long, *JHEP* **03**, 283 (2021), 2009.03828.
 [12] B. Salehian, M. A. Gorji, H. Firouzjahi, and S. Mukohyama, *Phys. Rev. D* **103**, 063526 (2021), 2010.04491.
 [13] M. Bastero-Gil, J. Santiago, R. Vega-Morales, and L. Ubaldi, *JCAP* **02**, 015 (2022), 2103.12145.
 [14] M. Gorghetto, E. Hardy, J. March-Russell, N. Song, and S. M. West, *JCAP* **08**, 018 (2022), 2203.10100.
 [15] T. Sato, F. Takahashi, and M. Yamada, *JCAP* **08**, 022 (2022), 2204.11896.
 [16] M. Redi and A. Tesi, *JHEP* **10**, 167 (2022), 2204.14274.
 [17] N. D. Barrie (2022), 2211.03902.
 [18] W. E. East and J. Huang, *JHEP* **12**, 089 (2022), 2206.12432.
 [19] D. Cyncynates and Z. J. Weiner (2023), 2310.18397.
 [20] A. Arvanitaki, S. Dimopoulos, M. Galanis, D. Racco, O. Simon, and J. O. Thompson, *JHEP* **11**, 106 (2021), 2108.04823.
 [21] M. B. Fröb, J. Garriga, S. Kanno, M. Sasaki, J. Soda, T. Tanaka, and A. Vilenkin, *JCAP* **1404**, 009 (2014), 1401.4137.
 [22] T. Kobayashi and N. Afshordi, *JHEP* **10**, 166 (2014), 1408.4141.
 [23] T. Hayashinaka, T. Fujita, and J. Yokoyama, *JCAP* **1607**, 010 (2016), 1603.04165.
 [24] M. Banyeres, G. Domènech, and J. Garriga, *JCAP* **1810**, 023 (2018), 1809.08977.
 [25] V. Domcke and K. Mukaida, *JCAP* **11**, 020 (2018), 1806.08769.
 [26] C. Stahl, *Nucl. Phys.* **B939**, 95 (2019), 1806.06692.
 [27] O. O. Sobol, E. V. Gorbar, and S. I. Vilchinskii, *Phys. Rev.* **D100**, 063523 (2019), 1907.10443.
 [28] V. Domcke, Y. Ema, and K. Mukaida, *JHEP* **02**, 055 (2020), 1910.01205.
 [29] O. O. Sobol, E. V. Gorbar, A. I. Momot, and S. I. Vilchinskii (2020), 2004.12664.
 [30] L. H. Ford, *Phys. Rev. D* **35**, 2955 (1987).
 [31] V. Kuzmin and I. Tkachev, *Phys. Rev. D* **59**, 123006 (1999), hep-ph/9809547.
 [32] M. Bastero-Gil, P. B. Ferraz, L. Ubaldi, and R. Vega-Morales (2023), 2311.09475.
 [33] S. Shakeri, M. A. Gorji, and H. Firouzjahi, *Phys. Rev. D* **99**, 103525 (2019), 1903.05310.
 [34] K. Nakayama (2020), 2004.10036.
 [35] M. Bastero-Gil and A. T. Manso (2022), 2209.15572.
 [36] P. D. Meerburg and E. Pajer, *JCAP* **1302**, 017 (2013), 1203.6076.

- [37] M. M. Anber and L. Sorbo, *Phys. Rev. D* **81**, 043534 (2010), 0908.4089.
- [38] N. Barnaby, E. Pajer, and M. Peloso, *Phys. Rev. D* **85**, 023525 (2012), 1110.3327.
- [39] N. Arkani-Hamed, L. Motl, A. Nicolis, and C. Vafa, *JHEP* **06**, 060 (2007), hep-th/0601001.
- [40] P. A. R. Ade et al. (Planck), *Astron. Astrophys.* **594**, A13 (2016), 1502.01589.
- [41] C. Di Paolo, F. Nesti, and F. L. Villante, *Mon. Not. Roy. Astron. Soc.* **475**, 5385 (2018), 1704.06644.
- [42] J. Alvey, N. Sabti, V. Tiki, D. Blas, K. Bondarenko, A. Boyarsky, M. Escudero, M. Fairbairn, M. Orkney, and J. I. Read, *Mon. Not. Roy. Astron. Soc.* **501**, 1188 (2021), 2010.03572.
- [43] P. A. R. Ade et al. (BICEP, Keck), *Phys. Rev. Lett.* **127**, 151301 (2021), 2110.00483.
- [44] M. Tristram et al., *Phys. Rev. D* **105**, 083524 (2022), 2112.07961.
- [45] A. Berlin, J. A. Dror, X. Gan, and J. T. Ruderman, *JHEP* **05**, 046 (2023), 2211.05139.
- [46] P. Agrawal, F.-Y. Cyr-Racine, L. Randall, and J. Scholtz, *JCAP* **05**, 022 (2017), 1610.04611.
- [47] R. Lasenby, *JCAP* **11**, 034 (2020), 2007.00667.
- [48] N. Siemonsen, C. Mondino, D. Egana-Ugrinovic, J. Huang, M. Baryakhtar, and W. E. East, *Phys. Rev. D* **107**, 075025 (2023), 2212.09772.